


Demonstration of the pathogenicity of a common non-exomic mutation in ABCA4 using iPSC-derived retinal organoids and retrospective clinical data

Erin R. Burnight^{1,2}, Beau J. Fenner^{1,2}, Ian C. Han^{1,2}, Adam P. DeLuca^{1,2}, S. Scott Whitmore^{1,2}, Laura R. Bohrer^{1,2}, Jeaneen L. Andorf^{1,2}, Elliott H. Sohn^{1,2}, Robert F. Mullins^{1,2}, Budd A. Tucker ^{1,2}, Edwin M. Stone^{1,2,*}

¹Institute for Vision Research, Carver College of Medicine, University of Iowa, 375 Newton Road, Iowa City, IA 52242, United States

²Department of Ophthalmology and Visual Sciences, Carver College of Medicine, University of Iowa, 200 Hawkins Drive, Iowa City, IA 52242, United States

*Corresponding author: Edwin M. Stone, Institute for Vision Research, Carver College of Medicine, University of Iowa, 375 Newton Road, Iowa City, IA 54422, United States. E-mail: edwin-stone@uiowa.edu

Abstract

Mutations in *ABCA4* are the most common cause of Mendelian retinal disease. Clinical evaluation of this gene is challenging because of its extreme allelic diversity, the large fraction of non-exomic mutations, and the wide range of associated disease. We used patient-derived retinal organoids as well as DNA samples and clinical data from a large cohort of patients with *ABCA4*-associated retinal disease to investigate the pathogenicity of a variant in *ABCA4* (IVS30 + 1321 A>G) that occurs heterozygously in 2% of Europeans. We found that this variant causes mis-splicing of the gene in photoreceptor cells such that the resulting protein contains 36 incorrect amino acids followed by a premature stop. We also investigated the phenotype of 10 patients with compound genotypes that included this mutation. Their median age of first vision loss was 39 years, which is in the mildest quintile of a large cohort of patients with *ABCA4* disease. We conclude that the IVS30 + 1321 A>G variant can cause disease when paired with a sufficiently deleterious opposing allele in a sufficiently permissive genetic background.

Keywords: *ABCA4*; Stargardt disease; retinal organoids; genetic testing; RNA splicing

Introduction

The *ABCA4* gene encodes a transmembrane protein that flips a phospholipid-bound vitamin A molecule from the intradiscal side of the outer segment disc membrane to the cytoplasmic side as an early step in the visual cycle [1, 2]. The gene is also expressed in the retinal pigment epithelium but the function of the protein in this cell type is less well understood [3].

Mutations in *ABCA4* are the most common cause of Mendelian retinal disease in outbred populations accounting for more than 17% of such patients [4]. The phenotype associated with these mutations ranges from a very severe cone-rod dystrophy that begins before five years of age and causes legal blindness before ten, to a much milder condition that mimics age-related macular degeneration with normal acuity persisting as late as the eighth decade of life.

The *ABCA4* gene has the sixth largest coding sequence among the 104 genes that cause the vast majority of inherited retinal disease [4] and it also exhibits a larger than average allelic diversity in the human population even when corrected for its large size [5]. For these reasons, many variants currently judged to be plausibly disease-causing in routine medical practice are so rare that there is very little statistical evidence to support their pathogenicity and the latter is simply inferred by their presence in patients with a convincing *ABCA4* phenotype and sometimes also by the demonstration that they lie on the allele opposite a more established disease-causing allele. Another challenge for the

molecular diagnosis of *ABCA4*-associated disease is that almost 20% of disease-causing mutations lie outside of the coding sequence and canonical splice sites [4] and for these deep intronic variants one does not even have the genetic code's predicted effect on the resultant protein as a guide to whether the variant is likely to be pathogenic or not.

In 2013, members of our group [6] used RNA sequencing data from human donor retina to identify *ABCA4* intronic sequences that are similar enough to canonical splice signals that the normal splicing machinery occasionally recognizes them, resulting in mis-spliced mRNAs. We hypothesized that sequence variations occurring near these signals would be more likely to cause pathogenic mis-splicing than mutations elsewhere in the gene's intronic DNA. We also used haplotype analysis of 28 unrelated individuals with clinical evidence of *ABCA4*-associated retinal disease but only a single detectable pathogenic mutation to look for evidence of non-exomic mutations that were shared among members of this cohort. Nine members of the cohort were also subjected to fragment-capture-based genomic sequencing of the entire *ABCA4* gene. We identified seven possible splice-altering variants among fourteen members of the one-allele cohort (50%) that were collectively present only once among 1392 control individuals; and, we were able to demonstrate mis-splicing *in vitro* for four of them. During the genomic sequencing phase of the Braun *et al.* study [6], we observed five additional non-exomic variants that were in *trans* to one or more patients' known

disease-causing alleles. At that time, we judged these variants to be too common in control individuals (e.g. 1% or more) to cause a rare Mendelian disease and as a result, we failed to recognize that one of these (IVS30 + 1321 A>G) was present in three of the 28 members (10.7%) of the one allele cohort.

In the present study, we used differentiated patient-derived induced pluripotent cells as well as DNA samples and clinical data from a larger cohort of patients with clinical ABCA4-associated retinal disease to demonstrate that the IVS30 + 1321 A>G variant (hereinafter referred to as IVS30 + 1321) is the most common deep intronic disease-causing mutation in the ABCA4 gene in this cohort and that its relatively mild impact on the gene's expression may require a permissive genetic background to become clinically manifest.

Results

Enrichment of IVS30 + 1321 among single allele patients

In 2013, we observed the IVS30 + 1321 variant heterozygously in three of 208 patients with a clinical phenotype compatible with ABCA4-associated disease but dismissed it as a non-disease-causing polymorphism because we also observed it in three of 200 control individuals ($p=1$). It was not until we performed a second genomic sequencing experiment and observed this variant in four of 22 patients *in trans* to their single known disease-causing ABCA4 allele that we were struck by how unlikely this was to occur by chance. That is, when a clinician masked to the patients' genotype separated these individuals from the general population based on their ABCA4 phenotype, and previous genetic testing separated them from the majority because of their single identified disease allele, the question became are there any variants among the 22 missing alleles that are enriched with respect to controls in a statistically unlikely manner? The presence of IVS30 + 1321 on four of these 22 alleles is statistically much greater than can be explained by chance ($p=3.3 \times 10^{-3}$ by Fisher's exact test).

Following this observation, we added the IVS30 + 1321 to our tiered genetic test for ABCA4 disease [4] and subsequently identified six additional individuals (10 total) with this variant *in trans* to a second plausible disease-causing mutation among a cohort of 460 patients with clinical evidence of ABCA4 disease. IVS30 + 1321 is the eleventh-most common disease-causing variation overall in this cohort (Fig. 1) and the most common deep intronic variant. It is noteworthy that most ABCA4 variants suspected to cause disease in this, or any cohort are present only once (Fig. 1). The only reason to suspect that these rare variants cause disease is that they lie on an allele opposite another plausible disease-causing variant in the gene and they are predicted to alter the encoded protein in some manner, often changing a single amino acid. In the case of the IVS30 + 1321, the prediction is that it would affect the ABCA4 protein by mis-splicing of the mRNA; a prediction that can be tested *in vitro* using patient-derived induced pluripotent stem cells (iPSCs).

ABCA4 expression in iPSC-derived retinal organoids

To evaluate the pathogenicity of the IVS30 + 1321 allele, iPSCs were generated from an individual (P2; Table 1, Supplementary Fig. 1A and B) carrying the IVS30 + 1321 variant on one allele and the previously described pathogenic IVS30-10 T>C variant on the opposite allele [7-9]. As a control, iPSCs from a normal disease-free individual (homozygous A at the IVS30 + 1321

position) were used. Because ABCA4 is localized to photoreceptor outer segments, and its mRNA is not robustly expressed prior to 75 days of differentiation, generation of mature retinal organoids was required to model the molecular phenotype of the IVS30 + 1321 variant. Three dimensional retinal organoids were generated using our previously published retinal differentiation protocol [7, 10, 11]. After 90 days of differentiation, retinal organoids generated from both control and proband iPSCs contained photoreceptor precursor cells expressing the markers OTX2, NRL, NR2E3, RCVRN, and OPN1SW (Fig. 2A-E). By differentiation day 140, OTX2 and cone arrestin (ARR3)-positive photoreceptor cells (Fig. 2B-F) extended outer-segment-like projections that were clearly visible via phase microscopy (Fig. 2F-H). To compare levels of photoreceptor cell gene expression between control- and proband-derived retinal organoids during development, quantitative PCR analysis was used. As retinal organoids developed, expression of the photoreceptor cell markers CRX, RCVRN, and ARR3 increased to similar levels in both control (Fig. 2J) and patient organoids (Fig. 2K). Importantly, at differentiation day 140 the level of ABCA4 transcript expression was not significantly different between patient and control (Fig. 2L).

Taken together, these data indicate that iPSC-derived retinal organoids from patients carrying the IVS30 + 1321 A>G variant develop normally and contain mature photoreceptor cells with outer segments that express ABCA4 transcript at similar levels to control.

Molecular phenotype of intronic ABCA4 variant IVS30 + 1321

Several disease-causing variants in ABCA4 are located within introns and contribute to retinal disease through aberrant splicing [5, 6, 12]. To determine if the IVS30 + 1321 variant in the proband alters splicing, we used PCR to amplify across intron 30 in control and patient cDNA isolated from iPSC-derived retinal organoids. We shotgun cloned these PCR products into pCR2.1-TOPO-TA plasmids and performed Sanger sequencing using primers located within the plasmid sequence to obtain full-length amplicon data. A splice variant containing 345 bp of intron 30 (hereinafter referred to as exon 30.1) was identified in retinal organoid cDNA obtained from P2 (2/137 clones) but not from the normal control (0/90 clones) (Supplementary Fig. 2). Inclusion of exon 30.1 results in a frameshift and introduction of a premature stop codon 36 amino acids downstream. To quantify exon 30.1 expression, RNA was isolated from 140-day retinal organoids and subjected to TaqMan[®] quantitative PCR analysis. TaqMan[®] assays targeting exons 4-5 and 49-50 were used to quantify total ABCA4 expression. A TaqMan[®] assay targeting the exon 30.1 sequence was used to quantify exon 30.1 inclusion. Using this strategy, which is much more sensitive than the Sanger sequencing of cloned PCR products described above, we observed very low levels of exon 30.1 in the disease-free control and a greater than two-fold increase in exon 30.1 expression in P2 (Fig. 2M). To validate these findings, iPSC-derived retinal organoids were generated from an additional patient (P1; Table 1, Fig. 3A-F) carrying the IVS30 + 1321 variant. By 140 days of differentiation, retinal organoids contained OTX2, cone arrestin (ARR3), recoverin, and rhodopsin-positive photoreceptor cells with outer-segment-like projections clearly visible via phase microscopy (Fig. 3A-C) and immunofluorescence (Fig. 3D-F). As per patient 1 above, retinal organoids expressed the genes RCVRN, RHO, ARR3 and ABCA4 at similar levels to those generated from a disease-free control individual (Fig. 3G). TaqMan[®] quantitative PCR analysis

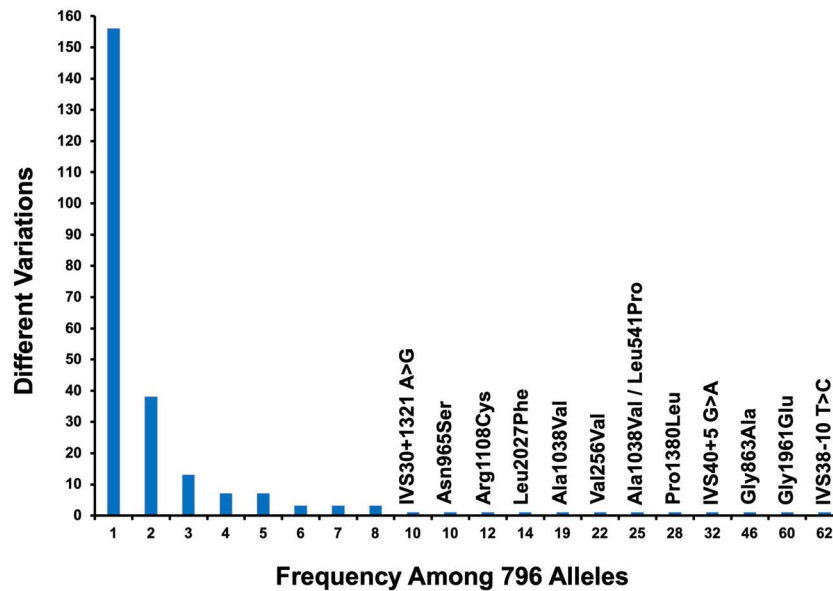


Figure 1. Allelic diversity of ABCA4. This figure shows the number of different disease-causing ABCA4 variants (y-axis) that occur at each frequency (x-axis) in a cohort of 390 probands with clinical features of ABCA4 disease. The unshared alleles of sixteen pseudo-dominant relatives are also included for a total of 796 alleles. Variants seen ten or more times in the cohort are specifically labeled. Of the 242 different plausible disease-causing variants seen in this cohort, 156 (64.5%) were observed only once.

Table 1. Summary of patients with IVS30 + 1321 on one allele.

	Gender	Age at First Vision Loss	Second Allele Variation	Second Allele c.DNA
P1	F	17	Asn1442Lys AAC>AAA	c.4326C>A
P2	F	18	IVS38-10 T>C	c.5461-10 T>C
P3	F	26	Ala1038Val GCC>GTC/Leu541Pro CTA>CCA	c.3113C>T/c.1622T>C
P4	M	>32	Asn965Ser AAT>AGT	c.2894A>G
P5	M	39	Gly1977Ser GGC>AGC	c.5929G>A
P6	F	40	Asn965Ser AAT>AGT	c.2894A>G
P7	M	41	Thr1526Met ACG>ATG	c.4577C>T
P8	M	56	Leu2027Phe CTC>TTC	c.6079C>T
P9	M	63	Thr1526Met ACG>ATG	c.4577C>T
P10	M	64	Gly607Arg GGG>AGG	c.1819G>A

revealed a greater than two-fold increase in expression of exon-30.1-containing ABCA4 transcript in P1 (Fig. 3H).

To ensure that these findings were not simply due to differences in developmental kinetics, the number of photoreceptor cells present in patient as compared to the disease-free controls was counted. Specifically, immunohistochemistry was performed and the percentage of cells expressing the rod and cone photoreceptor precursor cell marker OTX2 (Supplementary Fig. 3A) and the cone photoreceptor cell marker ARR3 (Supplementary Fig. 3B) were determined. There was no significant difference in the number of photoreceptor cells present in organoids derived from either patient (P1 and P2) or the disease-free controls (C1 and C2) (Supplementary Fig. 3A and B). To demonstrate that retinal organoids are not undergoing degeneration that could skew interpretation of our molecular findings, differentiation was extended for an additional 60 days, beyond the point of rod and cone photoreceptor cell genesis [13]. Given that patients with the mild IVS30 + 1321 A>G have late onset disease, it was not surprising that no significant difference in retinal organoid structure was detected following further organoid maturation (Supplementary Fig. 3C–F).

It was previously shown that mild splice variants such as IVS30 + 1321 when paired with a severe allele *in trans* can

produce mature RPE cells with similar levels of ABCA4 transcripts as that of unaffected individuals [14, 15]. Indeed, we could readily generate cultures of iPSC-derived RPE from a disease-free control (control 2) and patients 1 and 2 that were pigmented, formed ZO-1 positive tight junctions, and were morphologically indistinguishable from each other (Fig. 4A–F). In addition, there was no significant difference in expressed levels of the RPE cell transcripts *MITF*, *CRALBP*, and *BEST1* (Fig. 4G–I). To determine if iPSC-derived RPE cells express the same ABCA4 transcript as neural retina, Sanger sequencing of overlapping rt-PCR fragments was performed. While less abundant, the ABCA4 transcript expressed in iPSC-derived RPE was confirmed to be the same as that expressed in human donor retina and iPSC-derived retinal organoids (Supplementary Fig. 4).

To determine if the IVS30 + 1321 A>G variant induced the same splicing defect in RPE as it does in the neural retina, expression of exon 30.1 as a function of total ABCA4 transcript was evaluated using the above described TaqMan® qPCR assay. As shown in Fig. 4J, we observed greater than 3.5-fold increase in exon 30.1 expression in P1 and greater than 2-fold increase in exon 30.1 expression in P2 as compared to the disease-free control (C2; homozygous A at the IVS30 + 1321 position). Taken together, these data demonstrate a qualitative molecular pathogenic

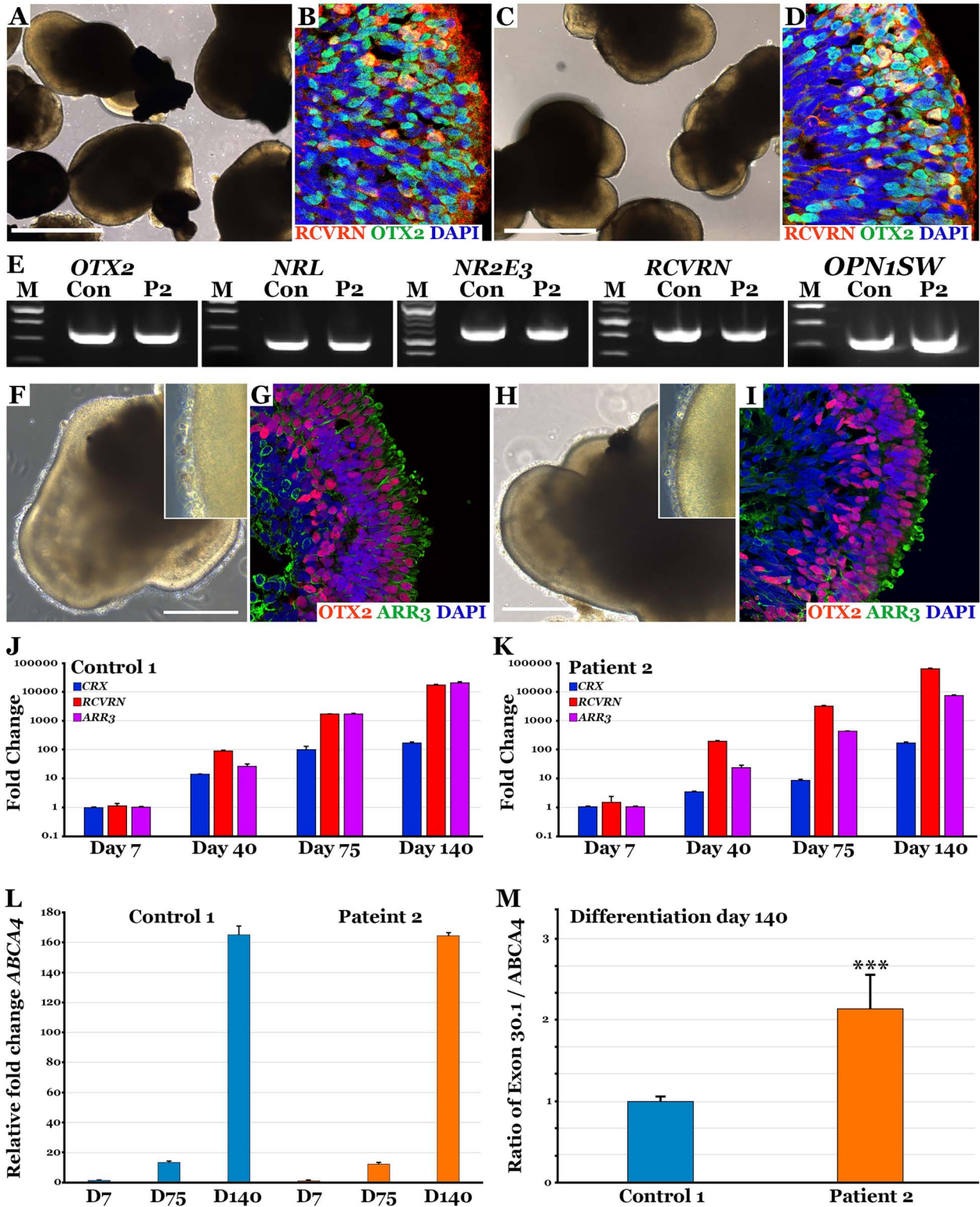


Figure 2. Presence of the IVS30 + 1321 A>G variant increases the rate of pseudo exon 30.1 inclusion in patient iPSC-derived retinal organoids. (A–D) Phase (A and C) and immunohistochemical (B and D) analysis of iPSC-derived retinal organoids (≥ 10 per line) from a control individual (A–B) and patient P2 (C–D) at 90-days of differentiation. (E) rt-PCR analysis targeted against the photoreceptor cell markers *OTX2*, *NRL*, *NR2E3*, *RCVRN* and *OPN1SW* at 90-days of differentiation. (F–I) Phase (A and H) and immunohistochemical (G and I) analysis of iPSC-derived retinal organoids (≥ 10 per line) from a control individual (F–G) and the proband (H–I) at 140-days of differentiation. (J and K) Quantitative PCR analysis of control (J) and proband (K) retinal organoids (≥ 10 per line) using TaqMan probes targeted against the photoreceptor cell markers *CRX*, *RCVRN*, and *ARR3*, at differentiation day 7, 40, 75 and 140, showing normal photoreceptor development. (L) Quantitative PCR analysis of control and proband retinal organoids using TaqMan probes targeted against *ABCA4*, at differentiation day 7, 75 and 140. (M) Quantitative PCR analysis of control and patient retinal organoids (≥ 10 per line) using TaqMan probes targeted against *ABCA4* pseudo exon 30.1 at differentiation day 140. Data is expressed as a ratio of exon 30.1 to total *ABCA4* (probes targeting exons 4–5 and 49–50). Despite normal development and near identical levels of *ABCA4* expression, iPSC-derived retinal organoids obtained from the proband express greater than two-fold more pseudo exon 30.1 than those obtained from an unaffected control.

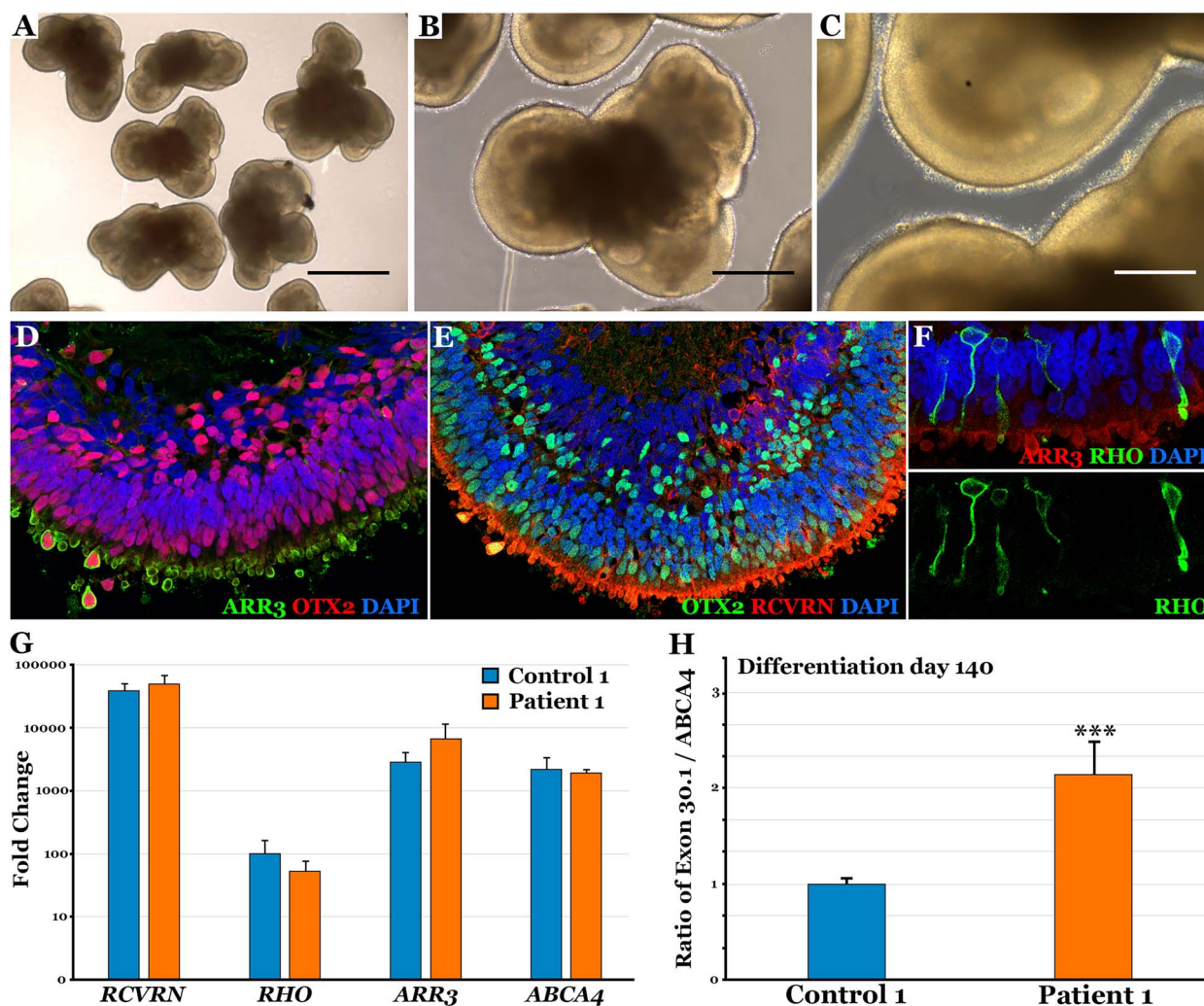


Figure 3. Presence of the IVS30 + 1321 A>G variant increases the rate of pseudo exon 30.1 inclusion in iPSC-derived retinal organoids generated from a second individual. (A–C) Phase micrographs depicting iPSC-derived retinal organoids (≥ 10 per line) from an additional patient (P1) with IVS30 + 1321 at 140-days of differentiation. By 140 days of differentiation retinal organoids contain photoreceptor cells with outer segment projections. (D–F) Immunocytochemical analysis of P1 iPSC-derived retinal organoids (≥ 10) at 140-days of differentiation (D: ARR3, OTX2, DAPI. E: OTX2, RCVRN, DAPI. F: RHO, ARR3, DAPI). (G) Quantitative PCR analysis of control and proband 2 iPSC-derived retinal organoids (≥ 10 per line) at 140 days of differentiation using TaqMan probes targeted against RCVRN, RHO, ARR3 and ABCA4. Data are expressed as fold change relative to day 0. (H) Quantitative PCR analysis of control and proband 2 retinal organoids (≥ 10 per line) using TaqMan probes targeted against ABCA4 pseudo exon 30.1 at differentiation day 140. Data is expressed as a ratio of exon 30.1 to total ABCA4. Despite normal development and near identical levels of ABCA4 expression, iPSC-derived retinal organoids obtained from proband 2 express greater than two-fold more pseudo exon 30.1 than those obtained from an unaffected control.

phenotype of the common IVS30 + 1321 ABCA4 variant in both retinal organoids and RPE generated from patients with clinically diagnosed ABCA4-associated macular dystrophy.

Mechanism of IVS30 mis-splicing

The pseudo-exon 30.1 has been reported in alternative transcripts expressed by several ABCA4 alleles carrying known pathogenic variants in intron 30 [6, 16–19]. It was previously suggested that exon 30.1 inclusion is likely due to creation of exonic splicing enhancers [19]. To determine if the IVS30 + 1321 A>G variant carried by P2 would be predicted to alter splice factor binding and exon 30.1 inclusion, we employed *in silico* prediction analysis using RBPmap (<http://rbpmap.technion.ac.il/> [20, 21]. RBPmap uses experimentally defined RNA binding motifs reported in the literature as either a consensus or Position Specific Scoring Matrix to predict protein binding to a given sequence based on a Weighted-Rank approach [22]. When we compared predicted binding sites containing the variant nucleotide (A or G), five were

predicted to have differential binding probabilities that varied by at least one log unit between alleles (Supplementary Fig. 5). The G allele (carried by P1 and P2) destroys predicted binding of three proteins and creates predicted binding of one protein (Supplementary Fig. 5). Of the three RNA binding proteins whose binding sites are disrupted by the IVS30 + 1321 A>G substitution, Splice Factor 1 (SF1), is known to silence alternative splicing [23].

Clinical features of IVS30 + 1321 patients

The demographics, genotypes and clinical features of the ten patients in our ABCA4 disease cohort who harbor the IVS30 + 1321 variant are summarized in Table 1, Fig. 5 and Supplementary Fig. 1. Three of the patients (P1–P3); experienced a loss of visual acuity before age 30 that was accompanied by a loss of foveal photoreceptors visible by optical coherence tomography (e.g. P1—Fig. 5A and B). One of the remaining eight was still asymptomatic at age 32 (P4—Fig. 5C and D) and the other seven first experienced symptoms between the ages of 40 and

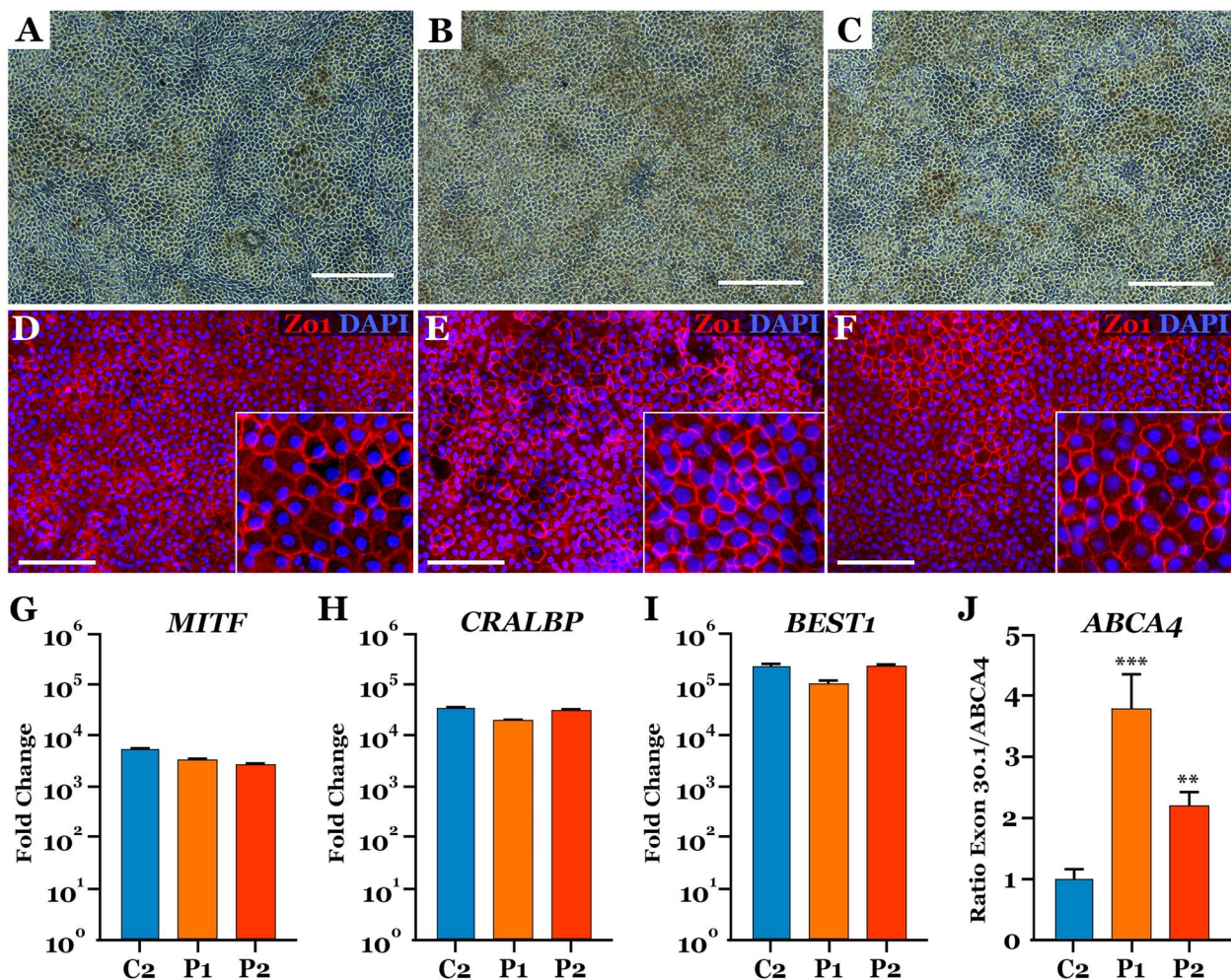


Figure 4. Patient-derived RPE differentiation. (A–C) Phase contrast images of patient-derived RPE cells (D80) from control (A) and two patients (P1—B and P2—C) carrying the IVS30 + 1321 A>G variant. Scale bars = 1000 μ m. (D and E) Immunocytochemical analysis of iPSC-derived RPE cells from control (D) and patients (P1—E and P2—F) at D80. ZO-1, DAPI. (G–J) rt-PCR analysis targeted against the RPE cell markers *MITF* (G), *CRALBP* (H), *BEST1* (I). Patient-derived RPE demonstrate ~ 3.5 and ~ 2 fold increased exon 30.1 inclusion (J), respectively. Error bars represent S.E.M. N = 3.

62 years. The phenotype of the latter eight was noteworthy in that the initial cellular dysfunction seemed to lie more at the level of the retinal pigment epithelium (RPE) and choriocapillaris than the cone photoreceptors. That is, the outer nuclear layer of the fovea was relatively spared in all eight of these individuals and the junctions of normal and atrophic RPE in the older members of this group (e.g. P9—Fig. 5E and F) were marked by outer retinal tubulations like those seen in choroideremia [24] and maternally inherited diabetes and deafness (MIDD) [25], suggesting that the RPE and choriocapillaris loss preceded the photoreceptor death [24].

The median age of first vision loss for the patients with an IVS30 + 1321 allele (39 years) is in the mildest quintile of the 460 patient *ABCA4* cohort suggesting that this allele is associated with greater residual *ABCA4* function than most. This idea is strengthened by the observation that none of the IVS30 + 1321 patients were homozygous for the allele nor were they compound heterozygotes with the known mild alleles Gly1961Glu or Gly863Ala [26]. The absence of the six possible combinations of these three alleles from the cohort of 390 probands with *ABCA4*-associated retinal disease is very unlikely to occur by chance ($p = 1.2 \times 10^{-8}$) and suggests that these six genotypes result in sufficient *ABCA4* function to prevent detectable disease in most individuals who harbor them.

IVS30 + 1321 is a complex allele

In most genes, there are numerous examples of more than one departure from the consensus human sequence occurring on the same allele and in some cases there is clear evidence that these variants affect the resulting protein in an additive manner. For example, in *ABCA4*, the combination of Leu541Pro with Ala1038Val is more deleterious allele than Ala1038Val by itself, and Leu541Pro does not exist by itself at any measurable frequency [27]. Since the initial molecular evaluation of Stargardt patients in the late 1990s, most investigators have considered the very common variant in *ABCA4* codon 1868 (Asn1868Ile; carrier frequency of 12.8% of non-Finnish Europeans) to be a non-disease-causing polymorphism. However, because this variant is noticeably enriched among patients with *ABCA4*-associated retinal disease, some authors have begun to reevaluate its possible involvement in retinal degeneration [28, 29]. During the present study, we noticed that all ten IVS30 + 1321 patients also harbored the Asn1868Ile variant and so we assessed all 390 probands of our *ABCA4* disease cohort and 608 of their family members to further investigate the relationship between these variants and other disease-causing mutations in *ABCA4* (Table 2). We also used the variant co-occurrence tool in the gnomAD database browser [27] to evaluate the relationship between the Asn1868Ile variant

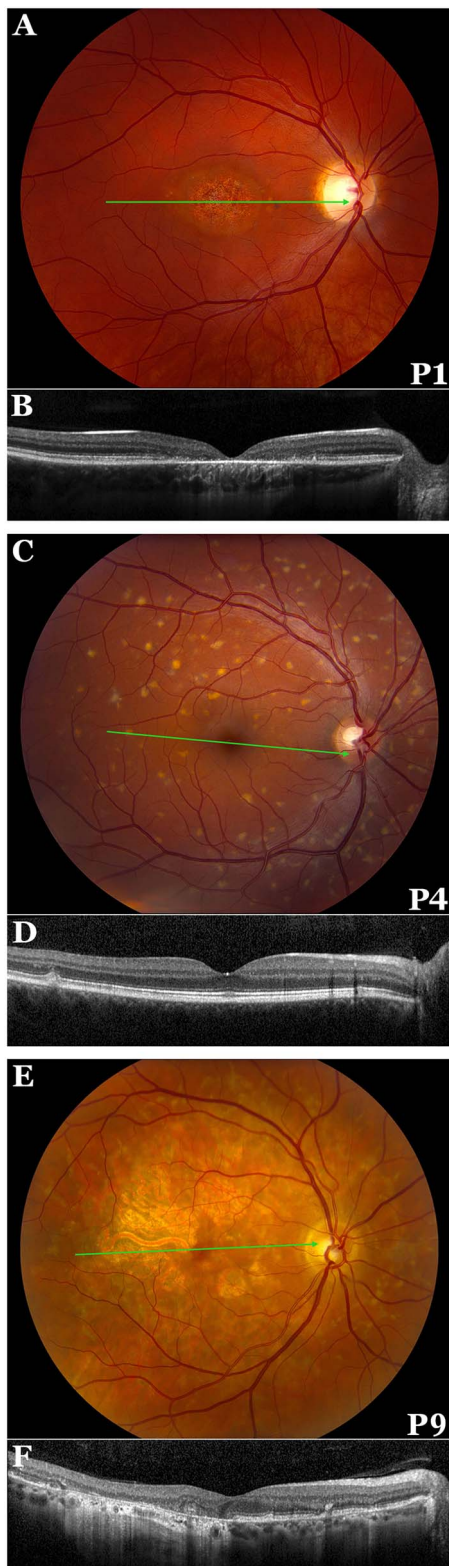


Figure 5. Color fundus photography and OCT obtained from patients with IVS30 + 1321. (A) Color fundus photograph of the right eye of P1, a 27-year-old woman with 20/100 acuity. There is an oval zone of atrophy with a shiny base centered on the foveola and ringed by a few small yellow flecks. (B) OCT of the right eye of P1 reveals central outer retinal loss and an RPE hypertransmission defect corresponding to the atrophy seen on the fundus image. (C) Color fundus photograph of the right eye of P4, a 30-year-old man with 20/15 acuity. There are numerous bright yellow flecks throughout the posterior pole that spare the central 1.5 mm. (D) OCT of the right eye of P4 shows intact retinal layers except for two

and other disease-causing coding sequence variants in the cohort (Table 2).

The Asn1868Ile variant was present on 179/796 alleles (22.5%) among the 390 probands and 16 unshared alleles of pseudo-dominant relatives in the cohort, which is much higher than its allele frequency in any well-studied human population (e.g. 6.6% in non-Finnish Europeans). However, at least 147 of these instances (82.1%) were in cis with another plausible disease-causing variation, all 22 of which are rarer in the general population than Asn1868Ile (Table 2). For example, Gly863Ala, which is one of the most common disease-causing mutations in any cohort of patients with ABCA4 disease (Table 1), was present in 44 probands in our cohort (11.3%) and every instance of this variation was in cis with Asn1868Ile. In contrast, in the general population, three fourths of the instances of Gly863Ala occurred on alleles without Asn1868Ile (Table 2). Thus, it appears that Gly863Ala cannot cause disease by itself but requires the Asn1868Ile variant for the allele to be pathogenic.

We do not know at present whether the Asn1868Ile variant is ever pathogenic without some other variant in cis to further injure the allele. We looked for the Asn1868Ile allele among 457 unaffected family members of the probands in our cohort and found it in trans with a disease-causing mutation in 21 asymptomatic adults (Supplementary Table 1). In eleven of these cases, the asymptomatic adult was more than 10 years older than the proband's age at first vision loss and the allele in trans to Asn1868Ile was the more severe of the probands two alleles (e.g. Gln1412Stop, Trp439Stop, Val256Val, IVS38-10, Pro1380Leu).

Discussion

The molecular diagnosis of ABCA4-associated retinal disease is among the most challenging in molecular ophthalmology. The amount of variation in this gene is extraordinary, perhaps a vestige of evolution's response to differing amounts of dietary vitamin A available to different human populations. Most normal individuals harbor multiple departures from the consensus human ABCA4 sequence and the pathogenicity or non-pathogenicity of a given allele results from the additive effect of all the variants scattered in cis across the more than 250 000 base pairs of the ABCA4 gene. Most ophthalmologists are largely unaware of the degree of normal variation that exists in the ABCA4 gene because much of the clinical testing performed over the past 25 years has not included the noncoding parts of the gene. Even when noncoding variants have been detected, their specific parental origin is often not established.

The tremendous range of genetic variation in the ABCA4 gene results in a similar diversity of ABCA4 protein function ranging from normal to none. Hypomorphic alleles that encode near-normal ABCA4 proteins have three clinically recognizable properties: 1) they do not cause disease homozygously or in combination with other hypomorphic alleles; 2) they are noticeably more common in the general population than null mutations (i.e. nonsense mutations, frameshift mutations and large deletions); and 3) the phenotypes of patients who harbor these alleles tend to be milder than the phenotypes of patients who harbor two alleles capable of causing disease homozygously. The IVS30 + 1321/Asn1868Ile allele that is the focus of this report exhibits all three of these hypomorphic features. Even though this allele is present in as much as 2% of normal individuals in some ethnicities (e.g. non-Finnish Europeans), none of the ten patients in our cohort who harbor this allele are homozygous for it nor are they compound heterozygotes with the most well-known hypomorphic alleles

Gly1961Glu and Gly863Ala/Asn1868Ile. The phenotype associated with the IVS30 + 1321/Asn1868Ile is quite mild, with most individuals remaining asymptomatic until their fourth decade of life. Furthermore, their disease appears to manifest at the level of the RPE. We believe that this is because the rate at which the toxic bisretinoid A2E is being produced in photoreceptor outer segments is low enough that outer segment turnover alone prevents A2E from accumulating within the cell body and killing photoreceptor cells directly. However, after many years of RPE phagocytosis of these bisretinoid-laden outer segments, the RPE cells ability to expel or process the A2E is overwhelmed, and the RPE succumbs. The death of the RPE then leads to a secondary loss of photoreceptor cells.

The relative allele frequencies of Gly1961Glu (60/796), Gly863Ala/Asn1868Ile (46/796) and IVS30 + 1321/Asn1868Ile (10/796) in our ABCA4 disease cohort are difficult to explain without invoking an additional modifying factor acting either in *cis* or *trans*. That is, since IVS30 + 1321/Asn1868Ile is almost twice as common in the general population as the other alleles combined (Table 2), one would expect it to have more than twice the opportunity to form disease-causing genotypes and to therefore be found in more than twice the number of patients in our cohort. Instead, IVS30 + 1321/Asn1868Ile was observed in one tenth the number of patients as those with Gly1961Glu or Gly863Ala/Asn1868Ile. It is possible that the ABCA4 protein encoded by IVS30 + 1321/Asn1868Ile has so much residual function that it only causes disease in the presence of a polymorphism in some other gene that augments the phenotype in some manner; for example, lowering the apoptotic threshold of the retinal pigment epithelium to bisretinoid accumulation. If such a *trans*-acting modifier was present in 5% of the population, it would account for the observed frequencies in our cohort. Alternatively, there might be two versions of the IVS30 + 1321/Asn1868Ile allele in the population, one 20 times less common than the other and differing by a currently undetected *cis* variation that additively weakens the encoded protein to the point that it is functionally equivalent to proteins encoded by Gly1961Glu or Gly863Ala/Asn1868Ile.

Of course, these hypotheses are not mutually exclusive; there may be multiple *cis*- and *trans*-acting modifiers of ABCA4 gene expression. The exciting thing is that cell biological and molecular methods are so advanced now that these possibilities are open to direct investigation. Additional *cis*-acting modifiers can be identified using approaches like the ones employed in the present study. A cohort of 30–50 probands can be assembled who have clinical features of ABCA4 disease, one plausible disease-causing allele and family members available for study. Genomic sequencing of the ABCA4 genes of three individuals per kindred can be performed to establish high-resolution haplotypes across the gene and the haplotypes in *trans* to the probands' known disease alleles can be scrutinized for variants that are enriched among the patients compared with controls. iPSCs from patients harboring these variants can then be used to investigate the mechanism by which these variants influence the expression of the ABCA4 protein.

Evidence for *trans*-acting modifiers can be sought in groups of patients with mild disease who harbor alleles that are significantly under-represented in the cohort. If one or more *trans*-acting modifiers is responsible for disease in these patients, one should be able to readily identify some unaffected siblings who share the proband's ABCA4 genotype. Finding the modifiers themselves will likely entail a candidate gene approach in which one uses knowledge of the pathophysiology of the disease to choose pathways such as the visual cycle where functional mutations would be most likely to augment or mitigate the disease and then informatively scrutinize these pathways in the whole-exome-sequencing data of mild phenotype patients, discordant siblings and controls looking for variants with frequencies that support the hypothesis. Candidate variants identified in this hypothesis-generating step could be validated (or not) using independent cohorts of similar patients. *Trans*-acting modifiers that vary in expression instead of protein sequence will be harder to identify, but one could do so by differentiating retinal and retinal pigment epithelial cells from the iPSCs of mild phenotype patients, discordant siblings and controls, and performing RNA sequencing to look for significant expression differences in candidate pathways and then validating the best candidate genes in a second independent cohort.

One might ask why it is important to sort out the details of these *cis* and *trans* modifiers of ABCA4. After all, most patients harbor two convincing alleles that behave in a reasonably predictable manner. From a scientific point of view, ABCA4 is a terrific model system for understanding oligogenic disease. The range of severity of the disease, the opportunity to examine the affected cells psychophysically, electrophysiologically and anatomically at near histopathological resolution in living patients, and the fact that ABCA4-associated disease is the most common Mendelian disorder affecting the retina all combine to make the modifier-seeking experiments more feasible than they would be in most other systems. From a treatment point of view, the gene itself is so large that virus-mediated gene replacement is not possible at present. If a modifier could be found that is responsible for the preservation of the fovea that we observe in some ABCA4 patients, perhaps the gene that encodes it will be small enough to deliver by AAV or its mechanism could be mimicked with a small molecule drug. From a molecular diagnosis point of view, it would be valuable to be able to explain some of the variation that we observe among patients with identical ABCA4 genotypes and by so doing come closer to a table of allele severities that would allow one to predict clinical outcomes from genotypes. It would also be very desirable to identify detectable *cis* variants that would resolve the discordance between the frequency of a putative disease allele and its frequency in patient cohorts. For example, as noted above, some authors have suggested that the Asn1868Ile variant by itself is pathogenic in some patients [28, 29]. This variant is more than 25 times as common in the population as Gly1961Glu and yet it is less common than Gly1961Glu in a large cohort of patients. It also occurs in *trans* to clearly pathogenic ABCA4 alleles in asymptomatic adults. We think that the most likely explanation for this is that there are a series of variants in *cis* with Asn1868Ile. One of these is the IVS30 + 1321 that is the subject of

hyperreflective deposits located between the ellipsoid band and the RPE. (E) Color fundus photograph of the right eye of P9, a 62-year-old man with 20/25-1 acuity. There is extensive macular RPE atrophy circumscribing the fovea with peninsular sparing of the foveal center. More peripherally there are numerous yellow flecks arranged in a reticular pattern, many of which are associated with hyperpigmentation and early atrophy. There is relative sparing of the peripapillary retina. (F) OCT of the right eye of P9 reveals temporal RPE and outer retinal atrophy with a zone of RPE hyper-transmission that reaches the fovea. The nasal retinal laminations are largely preserved with several small foci of incomplete outer retinal atrophy and pigment migration. The green arrow in the fundus photos (A, C, and E) represents the position of the OCT scan.

Table 2. Cohort and population frequencies of disease-causing ABCA4 variants in cis with Asn1868Ile.

Variant		Cohort			European (non-Finnish) Population (gnomAD)		
		With Asn1868Ile	Without Asn1868Ile	Total Alleles	With Asn1868Ile	Without Asn1868Ile	Total Alleles
Arg508Cys CGC>TGC	N	1	0	796	5	29	113 426
	%	0.1256%	0.0000%		0.0044%	0.0256%	
Gly863Ala (G)GA>(G)CA	N	46	0	796	227	686	113 550
	%	5.7789%	0.0000%		0.1999%	0.6041%	
Gly863Ala (G)GA>(G)CA/Arg572Gln CGA>CAA	N	3	0	796	N/A ^a	N/A ^a	N/A ^a
	%	0.3769%	0.0000%				
Gly863Ala (G)GA>(G)CA/Arg2030Stop CGA>TGA	N	2	0	796	N/A ^a	N/A ^a	N/A ^a
	%	0.2513%	0.0000%				
Ala1038Val GCC>GTC	N	1	18	796	14	239	113 538
	%	0.1256%	2.2613%		0.0123%	0.2105%	
Leu1201Arg CTG>CGG	N	1	4	796	1	12	105 230
	%	0.1256%	0.5025%		0.0010%	0.0114%	
Cys1490Tyr TGC>TAC	N	3	0	796	15	0	107 706
	%	0.3769%	0.0000%		0.0139%	0.0000%	
Asp1532Asn GAC>AAC	N	1	0	796	1	2	113 652
	%	0.1256%	0.0000%		0.0009%	0.0018%	
Val1725 ins1gtG	N	2	1	796	1	0	109 244
	%	0.2513%	0.1256%		0.0009%	0.0000%	
Val1854Leu GTG>TTG	N	1	0	796	0	6	113 622
	%	0.1256%	0.0000%		0	0.0053%	
Arg1898His GCG>CAC	N	1	0	796	16	277	113 598
	%	0.1256%	0.0000%		0.0141%	0.2438%	
IVS38-10 T>C	N	62	0	796	Non-Coding Variant	Non-Coding Variant	Non-Coding Variant
	%	7.7889%	0.0000%				
IVS30 + 1321 A>G	N	10	0	796	Non-Coding Variant	Non-Coding Variant	Non-Coding Variant
	%	1.2563%	0.0000%				
Tyr362Stop TAT>TAA	N	1	0	796	Not in gnomAD	Not in gnomAD	Not in gnomAD
	%	0.1256%	0.0000%				
Gly435Val GGG>GTG	N	2	0	796	Not in gnomAD	Not in gnomAD	Not in gnomAD
	%	0.2513%	0.0000%				
Gly1065Asp GGC>GAC	N	1	0	796	Not in gnomAD	Not in gnomAD	Not in gnomAD
	%	0.1256%	0.0000%				
Leu1070 ins2cTG	N	2	0	796	Not in gnomAD	Not in gnomAD	Not in gnomAD
	%	0.2513%	0.0000%				
His1118Asp CAC>GAC	N	1	0	796	Not in gnomAD	Not in gnomAD	Not in gnomAD
	%	0.1256%	0.0000%				
Thr1726Asn ACC>AAC	N	1	0	796	Not in gnomAD	Not in gnomAD	Not in gnomAD
	%	0.1256%	0.0000%				
Pro1776Leu CCC>CTC	N	1	0	796	Not in gnomAD	Not in gnomAD	Not in gnomAD
	%	0.1256%	0.0000%				
Gly1886Glu GGG>GAG	N	1	0	796	Not in gnomAD	Not in gnomAD	Not in gnomAD
	%	0.1256%	0.0000%				
Leu1943Pro CTA>CCA	N	1	0	796	Not in gnomAD	Not in gnomAD	Not in gnomAD
	%	0.1256%	0.0000%				

^aThe relationship among 3 variants can't be evaluated with this tool in gnomAD.

this paper, another is Gly863Ala, more than a dozen others are shown in Table 2, and several more are yet to be discovered. Until the ABCA4 modifier landscape can be significantly clarified, we

think it best to confine one-allele molecular diagnoses to non-hypomorphic alleles whose frequencies in patient cohorts match their frequencies in the general population.

Materials and methods

Human subjects

Between November, 1986 and August, 2022, most patients seen in the Retina Clinic of the University of Iowa who were suspected to have a Mendelian retinal disease were offered participation in a long-term study designed to identify the molecular cause of their condition. After written informed consent was obtained, venous blood samples were obtained from the more than 12 000 patients and selected family members who agreed to participate. DNA was extracted from these samples and subjected to a phenotypically-focused tiered testing strategy beginning with allele-specific testing of the most common disease alleles and progressing through Sanger sequencing of candidate genes and in many cases to next generation sequencing of whole exomes and whole genomes as previously described [4]. 460 members of 390 families with clinical features of ABCA4 disease were found to harbor two ($n=400$) or one ($n=60$) plausible disease-causing alleles in ABCA4. Among the two allele patients, ten were found to harbor a variant in ABCA4 IVS30 (+1321 A>G) and these ten patients are the subject of this report.

Clinical assessment

The medical records of the ten IVS30+1321 patients were reviewed to determine the age at which they first experienced ABCA4-related vision loss. All individuals also had a complete eye examination including visual acuity assessment, slit-lamp biomicroscopy, and indirect ophthalmoscopy, Goldmann perimetry, color fundus photography, and spectral-domain optical coherence tomography.

Generation and characterization of patient derived induced pluripotent stem cells

Fibroblasts from two patients (P1 and P2) harboring the IVS30 + 1321 variant and one unrelated, disease-free control individual were isolated from skin biopsies taken from the upper non-sun-exposed arm as previously described [7–9]. iPSCs were generated by viral transduction of the transcription factors OCT4, SOX2, KLF4, and cMYC using the CytoTune™-iPS 2.0 Sendai Reprogramming Kit per manufacturer's instructions (Thermo Fisher Scientific). At 25–30 days following transduction, when newly generated iPSC colonies reach 1–2 mm in diameter, 12 iPSC colonies were manually dissected free from the surrounding cells, plated in separate wells of a LN521 (BioLamina) coated 12-well culture dish in Essential 8 medium (Thermo Fisher Scientific), and expanded for 10 passages as independent cell lines. iPSC pluripotency was confirmed using the TaqMan® Human Pluripotent Stem Cell Scorecard™ Panel (Thermo Fisher Scientific) according to manufacturer's protocol [30, 31]. Gene expression data were analyzed using the hPSC Scorecard™ Analysis Software (Thermo Fisher Scientific). Patient and control iPSC lines were confirmed to have a normal karyotype via a standard G-banding protocol as previously described [10, 32]. Following validation, a single cell line from each patient and disease-free control was used for subsequent differentiation experiments and all remaining clones were frozen for future use in the event that the selected line was determined to have a low capacity for retinal differentiation [15]. For all experiments presented, the data represent a minimum of 3 independent rounds of differentiation.

Derivation of retinal organoids

Differentiation of iPSCs into retinal organoids was performed through embryoid body (EB) formation as previously described

[7, 10, 11]. Briefly, iPSCs were dissociated into single cell suspension using TrypLE Express Enzyme Solution (Thermo Fisher Scientific) and counted using the Countess™ Automated Cell Counter (Thermo Fisher Scientific). iPSCs were plated in 96-well ultra-low adhesion sphere forming V-bottom tissue culture plates (1×10^4 cells/well; Corning Life Sciences) and transitioned from Essential 8 medium to neural induction medium [NIM—DMEM/F12 (1:1), 1% N2 Supplement, 1% non-essential amino acids, 1% Glutamax (Thermo Fisher Scientific), 2 $\mu\text{g/ml}$ heparin (Sigma) and 0.2% Primocin (Invivogen)] over a six-day time period. At day 6, EBs were cultured in NIM media containing recombinant human BMP4 (1.5 nM; R&D Systems). The following day, EBs from all 96 wells were transferred to Matrigel (Corning Life Sciences) coated 6-well culture dishes (96 EBs/well) to adhere in NIM+BMP4 media. BMP4 was transitioned out of NIM media over seven days. On day 16, media were changed to retinal differentiation medium (RDM—DMEM/F12 (3:1), 2% B27 Supplement, 1% non-essential amino acids, 1% Glutamax and 0.2% Primocin) and retinal organoids were cultured adherently for an additional 9–14 days. Following adherent outgrowth and maturation, organoids were mechanically lifted by spraying cells with media and transferred to ultra-low adhesion T25 flasks (Corning Life Sciences). Three-dimensional retinal organoids were maintained in 3D RDM [RDM, 10% FBS, 100 nM taurine (Sigma-Aldrich), 1:1000 chemically defined lipid supplement (Thermo Fisher Scientific), and 1 μM retinoic acid (Sigma-Aldrich)] and collected at a series of timepoints for RNA analysis. At day 100, retinoic acid was removed from the media to encourage outer segment growth. Organoids were cultured in this manner for the remainder of the study. Phase images were captured using an EVOS-XL microscope (Thermo Fisher Scientific). Data presented were obtained from at least three independent differentiations for each patient and disease-free control cell line.

Immunocytochemistry

Three-dimensional iPSC-derived retinal organoids (≥ 10 per line) at 90, 140, and 200 days post-differentiation were fixed in 4% PFA, cryopreserved using a sucrose gradient, and frozen in Optimal Cutting Temperature compound (VWR) for cryosectioning. The Leica CM1850 cryostat (Leica Microsystems) was used to section organoids at a thickness of 15 μm and transferred to Superfrost glass slides (Thermo Fisher Scientific). For iPSC-derived RPE cell analysis cells were cultured on Matrigel and poly-D-Lysine coated coverslips and fixed in 4% PFA. In both retinal organoid and RPE analysis, slides/coverslips were rinsed in PBS for 10 min and blocked with SuperBlock Blocking Buffer (Thermo Fisher Scientific) for 1 h at room temperature. Sections were labeled with the primary antibodies goat anti-OTX2 (1:100; R&D Systems), rabbit anti-recoverin (1:100; EMD Millipore), and rabbit anti-arrestin3 (1:100; LifeSpan Bio). Primary antibodies were detected using Alexa Fluor secondary antibodies donkey anti-goat AF488 (1:1000; Thermo Fisher Scientific), goat anti-rabbit AF647 (1:1000, Thermo Fisher Scientific), and donkey anti-goat AF568 (1:1000, Thermo Fisher Scientific). Cell nuclei were counterstained using DAPI. Stained retinal organoid sections were imaged using a Leica DM 2500 SPE confocal microscope (Leica Microsystems). For cell count analysis, images were coded and counted by a masked observer. Counts were obtained from 3 independent differentiations performed on different days.

PCR analysis

Total RNA was extracted from EBs and retinal organoids (≥ 10 per line) using the NucleoSpin RNA extraction kit (Clontech) following manufacturer's instructions. cDNA was generated with

SuperScript™ IV VILO™ Master Mix (Thermo Fisher Scientific) using 200 ng DNase-treated (RQ1 DNase; Promega Corporation) RNA following manufacturer's protocols. ABCA4 and retinal marker transcripts were amplified (100 ng cDNA template) using BIOLASE DNA polymerase (Bioline) and electrophoresed on 2% E-gels (Thermo Fisher Scientific). TaqMan gene expression assays detecting ABCA4 exons 4–5 (Thermo Fisher Scientific Cat. # Hs00979595_m1), exons 49–50 (Thermo Fisher Scientific Cat. # Hs00979594_m1), and exon 30.1 (Thermo Fisher Scientific Custom Design Cat. # APAAGTP IVS30 FAM) were used to quantify ABCA4 expression in retinal organoids. Expression was normalized to GUSB (Thermo Fisher Scientific Cat. # Hs00939627). Gene expression was quantified using the QuantStudio 3 Real-Time PCR System (Thermo Fisher Scientific) using the relative quantification method with TaqMan Fast Advanced Master Mix according to the manufacturer's instructions. Primer and probes used are listed in [Supplementary Table 2](#).

Statistics

When calculating allele frequencies in the ABCA4 disease cohort, only the alleles of probands (n=390) and the unshared alleles of pseudodominant cases (n=16) were included. The carrier frequency of the IVS30+1321 in ABCA4 patients versus controls was assessed using Fisher's exact test. The likelihood that by chance, neither Gly863Ala/Asn1868Ile, Gly1961Glu, nor IVS30+1321 would ever occur homozygously or compound heterozygously with either of the other two alleles in our cohort of 390 probands with ABCA4 disease was calculated by first subtracting their combined allele frequencies among our ABCA4 probands (0.14572) from one to yield the probability of being paired with any other allele in the cohort (0.85427) and then raising this quantity to the 116th power, corresponding to the 116 opportunities these heterozygous alleles had to be paired with one another in the cohort. The result is 1.2×10^{-8} .

For the iPSC experiments reported in [Figs 2 and 3](#), a two-tailed unpaired Student's T-test was performed. ** = $P < 0.01$.

Study approval

This study was approved by the institutional review board of the University of Iowa and adhered to the tenets set forth in the Declaration of Helsinki. Written informed consent was obtained from all subjects prior to participation.

Supplementary data

[Supplementary data](#) is available at *HMG Journal* online.

Conflict of interest statement: The authors declare no conflicts of interest in completing this work.

Funding

This work was supported, in part, by the University of Iowa Institute for Vision Research and the National Eye Institute P30 EY025580 and 1R01 EY033331.

Data availability

All data on which the conclusions of the paper rely are provided. Further information including software code will be made available to readers upon request.

References

- Weng J, Mata NL, Azarian SM. et al. Insights into the function of Rim protein in photoreceptors and etiology of Stargardt's disease from the phenotype in abcr knockout mice. *Cell* 1999;**98**:13–23.
- Quazi F, Lenevich S, Molday RS. ABCA4 is an N-retinylidene-phosphatidylethanolamine and phosphatidylethanolamine importer. *Nat Commun* 2012;**3**:925.
- Lenis TL, Hu J, Ng SY. et al. Expression of ABCA4 in the retinal pigment epithelium and its implications for Stargardt macular degeneration. *Proc Natl Acad Sci U S A* 2018;**115**:E11120–7.
- Stone EM, Andorf JL, Whitmore SS. et al. Clinically focused molecular investigation of 1000 consecutive families with inherited retinal disease. *Ophthalmology* 2017;**124**:1314–31.
- Webster AR, Heon E, Lotery AJ. et al. An analysis of allelic variation in the ABCA4 gene. *Invest Ophthalmol Vis Sci* 2001;**42**:1179–89.
- Braun TA, Mullins RF, Wagner AH. et al. Non-exomic and synonymous variants in ABCA4 are an important cause of Stargardt disease. *Hum Mol Genet* 2013;**22**:5136–45.
- Wiley LA, Burnight ER, DeLuca AP. et al. cGMP production of patient-specific iPSCs and photoreceptor precursor cells to treat retinal degenerative blindness. *Sci Rep* 2016;**6**:30742.
- Tucker BA, Mullins RF, Streb LM. et al. Patient-specific iPSC-derived photoreceptor precursor cells as a means to investigate Retinitis pigmentosa. *eLife* 2013;**2**:e00824.
- Tucker BA, Anfinson KR, Mullins RF. et al. Use of a synthetic xeno-free culture substrate for induced pluripotent stem cell induction and retinal differentiation. *Stem Cells Transl Med* 2013;**2**:16–24.
- Sharma TP, Wiley LA, Whitmore SS. et al. Patient-specific induced pluripotent stem cells to evaluate the pathophysiology of TRNT1-associated Retinitis pigmentosa. *Stem Cell Res* 2017;**21**:58–70.
- Small KW, DeLuca AP, Whitmore SS. et al. North Carolina macular dystrophy is caused by dysregulation of the retinal transcription factor PRDM13. *Ophthalmology* 2016;**123**:9–18.
- Zernant J, Schubert C, Im KM. et al. Analysis of the ABCA4 gene by next-generation sequencing. *Invest Ophthalmol Vis Sci* 2011;**52**:8479–87.
- Mullin NK, Bohrer LR, Voigt AP. et al. Loss of NR2E3 disrupts rod photoreceptor cell maturation causing a fate switch late in human retinal development. *J Clin Invest*. 2024;**134**(11):e173892. <https://doi.org/10.1172/JCI173892>.
- Farnoodian M, Bose D, Khristov V. et al. Cell-autonomous lipid-handling defects in Stargardt iPSC-derived retinal pigment epithelium cells. *Stem Cell Reports* 2022;**17**:2438–50.
- Matynia A, Wang J, Kim S. et al. Assessing variant causality and severity using retinal pigment epithelial cells derived from Stargardt disease patients. *Transl Vis Sci Technol* 2022;**11**:33.
- Khan M, Arno G, Fakin A. et al. Detailed phenotyping and therapeutic strategies for intronic ABCA4 variants in Stargardt disease. *Mol Ther Nucleic Acids* 2020;**21**:412–27.
- Bauwens M, Garanto A, Sangermano R. et al. ABCA4-associated disease as a model for missing heritability in autosomal recessive disorders: novel noncoding splice, cis-regulatory, structural, and recurrent hypomorphic variants. *Genet Med* 2019;**21**:1761–71.
- Garanto A, Duijkers L, Tomkiewicz TZ. et al. Antisense oligonucleotide screening to optimize the rescue of the splicing defect caused by the recurrent deep-intronic ABCA4 variant c.4539+2001 G>A in Stargardt disease. *Genes (Basel)* 2019;**10**:452.

19. Albert S, Garanto A, Sangermano R. et al. Identification and rescue of splice defects caused by two neighboring deep-intronic ABCA4 mutations underlying Stargardt disease. *Am J Hum Genet* 2018;**102**:517–27.
20. Paz I, Kosti I, Ares M Jr. et al. RBPmap: a web server for mapping binding sites of RNA-binding proteins. *Nucleic Acids Res* 2014;**42**:W361–7.
21. Paz I, Argoetti A, Cohen N. et al. RBPmap: a tool for mapping and predicting the binding sites of RNA-binding proteins considering the motif environment. *Methods Mol Biol* 2022;**2404**: 53–65.
22. Akerman M, David-Eden H, Pinter RY. et al. A computational approach for genome-wide mapping of splicing factor binding sites. *Genome Biol* 2009;**10**:R30.
23. Corioni M, Antih N, Tanackovic G. et al. Analysis of in situ pre-mRNA targets of human splicing factor SF1 reveals a function in alternative splicing. *Nucleic Acids Res* 2011;**39**:1868–79.
24. Zweifel SA, Engelbert M, Laud K. et al. Outer retinal tubulation: a novel optical coherence tomography finding. *Arch Ophthalmol* 2009;**127**:1596–602.
25. Han IC, Critser DB, Stone EM. Subliminal message outer retinal tubulations resembling mitochondria in maternally inherited diabetes and deafness. *Ophthalmol Retina* 2020;**4**:1102.
26. Wolf GK, Grychtol B, Boyd TK. et al. Regional overdistension identified with electrical impedance tomography in the perflubron-treated lung. *Physiol Meas* 2010;**31**:S85–95.
27. Karczewski KJ, Francioli LC, Tiao G. et al. The mutational constraint spectrum quantified from variation in 141,456 humans. *Nature* 2020;**581**:434–43.
28. Runhart EH, Sangermano R, Cornelis SS. et al. The common ABCA4 variant p.Asn1868Ile shows nonpenetrance and variable expression of Stargardt disease when present in trans with severe variants. *Invest Ophthalmol Vis Sci* 2018;**59**:3220–31.
29. Zernant J, Lee W, Collison FT. et al. Frequent hypomorphic alleles account for a significant fraction of ABCA4 disease and distinguish it from age-related macular degeneration. *J Med Genet* 2017;**54**:404–12.
30. Fergus J, Quintanilla R, Lakshmipathy U. Characterizing pluripotent stem cells using the TaqMan® hPSC Scorecard(TM) panel. *Methods Mol Biol* 2016;**1307**:25–37.
31. Tsankov AM, Akopian V, Pop R. et al. A qPCR ScoreCard quantifies the differentiation potential of human pluripotent stem cells. *Nat Biotechnol* 2015;**33**:1182–92.
32. Songstad AE, Wiley LA, Duong K. et al. Generating iPSC-derived choroidal endothelial cells to study age-related macular degeneration. *Invest Ophthalmol Vis Sci* 2015;**56**:8258–67.